

## Experimental characterization of single-walled carbon nanotube film-Si Schottky contacts using metal-semiconductor-metal structures

Ashkan Behnam,<sup>1</sup> Jason L. Johnson,<sup>1</sup> Yongho Choi,<sup>1</sup> M. Günhan Ertosun,<sup>2</sup> Ali K. Okyay,<sup>2</sup> Pawan Kapur,<sup>2</sup> Krishna C. Saraswat,<sup>2</sup> and Ant Ural<sup>1,a)</sup>

<sup>1</sup>Department of Electrical and Computer Engineering, University of Florida, Gainesville, Florida 32611, USA

<sup>2</sup>Department of Electrical Engineering, Stanford University, Stanford, California 94305, USA

(Received 26 November 2007; accepted 22 May 2008; published online 18 June 2008)

We demonstrate that single-walled carbon nanotube (CNT) films make a Schottky contact on silicon by experimentally characterizing metal-semiconductor-metal (MSM) structures. We find that at temperatures above 240 K, thermionic emission is the dominant transport mechanism across CNT film-Si contacts, and at lower temperatures tunneling begins to dominate. At high bias voltages, the CNT film MSM devices exhibit a higher photocurrent-to-dark current ratio relative to that of metal control devices. Our results not only provide insight into the fundamental electronic properties of the CNT film-Si junction but also opens up the possibility of integrating CNT films as Schottky electrodes in conventional Si-based devices. © 2008 American Institute of Physics.

[DOI: 10.1063/1.2945644]

A single-walled carbon nanotube (CNT) film is a three-dimensional film of tens of nanometer thickness, consisting of an interwoven mesh of single-walled nanotubes, exhibiting uniform physical and electronic properties independent of the diameter, chirality, location, and direction of individual tubes making up the film due to ensemble averaging.<sup>1-3</sup> Their low resistivity, high transparency in visible and near IR wavelengths,<sup>1</sup> and the ability to deposit and pattern them on a variety of substrates with high reliability and reproducibility<sup>2-5</sup> have established CNT films as a class of materials that can be used as transparent and conductive electrodes in a wide range of optoelectronic devices.<sup>6-10</sup>

Although the properties of CNT films and their contacts with organic materials<sup>7-9</sup> and III-V semiconductors<sup>6,10</sup> have recently been studied, the electronic properties of the junction between the CNT film and the most widely used and technologically important semiconductor, silicon, still remains unexplored. In this letter, we characterize the contact between CNT film and silicon by fabricating metal-semiconductor-metal (MSM) structures where the CNT film acts as the metal and Si is the semiconductor. This is in contrast to the application of CNT films as active semiconducting layers in thin film transistors. We demonstrate that the CNT film makes a Schottky contact to Si and extract its barrier height. We find that at temperatures above 240 K, thermionic emission is the dominant transport mechanism, and at lower temperatures tunneling begins to dominate. We also characterize the photoresponse of CNT film-Si MSM structures and compare their dark and photocurrent with standard metal-based control MSM devices. We find that at high bias voltages, the CNT film MSM devices exhibit a higher photocurrent-to-dark current ratio relative to that of the control devices, while maintaining a comparable responsivity. These results not only provide information about the fundamental electronic properties of the CNT film-Si junction but also demonstrate a conventional Si-based optoelec-

tronic device where the CNT film is integrated as a Schottky electrode.

MSM structures with CNT film electrodes were fabricated on lightly doped ( $10^{14}$ – $10^{15}$  cm<sup>-3</sup>) *n*- and *p*-type Si substrates, as shown in Figs. 1(a)–1(d). After the growth of a 400 nm thick thermal oxide, active area windows of various dimensions were etched in the oxide using HF [Fig. 1(b)]. This was followed by the deposition of an ~50 nm thick CNT film, prepared by vacuum filtration, as explained in detail previously.<sup>1,3</sup> The film exhibits metallic behavior with a resistivity on the order of  $10^{-4}$  Ω cm. An atomic force microscope (AFM) image of an as-prepared CNT film is shown Fig. 1(e). The CNT film was then patterned into interdig-

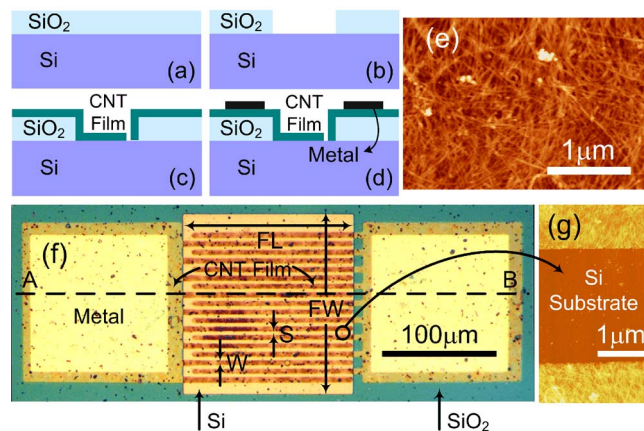


FIG. 1. (Color online) [(a)–(d)] Cross-sectional schematic of the fabrication process flow for the MSM structures with CNT film electrodes along the dashed line AB shown in part (f): (a) 400 nm thick SiO<sub>2</sub> isolation layer is thermally grown on the Si substrate. (b) Active area windows are opened in SiO<sub>2</sub> by photolithography and wet etching using HF. (c) ~50 nm thick CNT film is deposited on the substrate and patterned by photolithography and ICP etching. (d) Cr/Pd metal contacts are patterned on the nanotube film contact pads using photolithography, e-beam evaporation, and lift-off. (e) AFM image showing the texture of a 15 nm thick as-prepared CNT film. (f) Top view optical microscope image of a CNT film-Si MSM structure, showing the definition of various device dimensions. (g) AFM image showing the area between two CNT film electrode fingers of the MSM structure.

<sup>a)</sup> Author to whom correspondence should be addressed. Electronic mail: antural@ufl.edu.

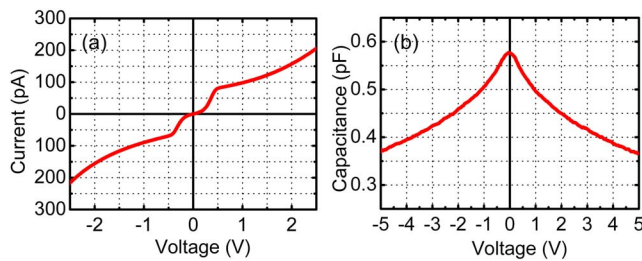


FIG. 2. (Color online) (a) Current-voltage and (b) capacitance-voltage characteristics measured at room temperature for a CNT film *n*-type Si MSM structure with  $FL=FW=300\ \mu\text{m}$  and  $W=S=50\ \mu\text{m}$ .

tated finger electrodes by photolithography and inductively coupled plasma (ICP) etching, as explained in detail previously<sup>3,4</sup> [Fig. 1(c)]. Finally, for electrical probing, a chromium/palladium metal stack was patterned on the CNT film contact pads [Fig. 1(d)]. Figure 1(f) shows an optical microscope image of a finished MSM device, illustrating the various device dimensions, such as active area width  $FW$ , finger length  $FL$ , finger width  $W$ , and finger spacing  $S$ . Figure 1(g) shows the AFM image of the area between two CNT film electrode fingers.

Figures 2(a) and 2(b) show the  $I$ - $V$  and  $C$ - $V$  characteristics (measured using a Keithley 4200 semiconductor characterization system and an HP 4294A impedance analyzer), respectively, at room temperature for a CNT film-Si MSM device with  $W=S=50\ \mu\text{m}$  and  $FL=FW=300\ \mu\text{m}$ . Other devices with different dimensions have resulted in similar characteristics. The data in Fig. 2 clearly exhibit the characteristic  $I$ - $V$  and  $C$ - $V$  curves of two back-to-back Schottky diodes,<sup>11</sup> demonstrating that the CNT film forms a Schottky contact on Si. Moreover, the symmetry of the  $I$ - $V$  and  $C$ - $V$  curves indicates that the two Schottky diodes are identical, confirming that the CNT film acts as a uniform electronic material.

The concave increase in the current and the appearance of a transition point at small voltages displayed in Fig. 2(a) are not expected for an ideal MSM device.<sup>11</sup> As previous studies on the current transport in metal-insulator-semiconductor-insulator-metal structures suggest, the existence of a thin layer of oxide between the CNT film and Si would result in an  $I$ - $V$  curve with a shape similar to that in Fig. 2(a).<sup>12</sup> Since the CNT film is porous, it is likely that native oxide forms at the CNT film-Si interface, resulting in the observed features in the  $I$ - $V$  curves. Since any native oxide that forms would be very thin, thermionic emission theory can still be used to analyze the transport across the CNT film-Si junction, as discussed below. Figure 2(a) also shows that the current does not saturate at high voltages, but rather increases monotonically with applied voltage. This could result from Schottky barrier lowering due to charge accumulation at surface states and due to the strong electric field at the edges of the electrodes<sup>13</sup> or individual nanotubes.

In order to extract the Schottky barrier height between the CNT film and Si, we have also measured the  $I$ - $V$  characteristics of several MSM devices as a function of temperature in a Lakeshore Cryotronics TTP4 low temperature probe station. Figure 3(a) shows the log  $I$ - $V$  curves of a CNT film-*p*-type Si MSM device at temperatures between 150 and 340 K. The Schottky barrier height of the CNT film-Si junction can be extracted from the slope of the Richardson plot of  $\log I/T^2$  versus  $1/T$  at a fixed voltage.<sup>11</sup> Figure 3(b) depicts

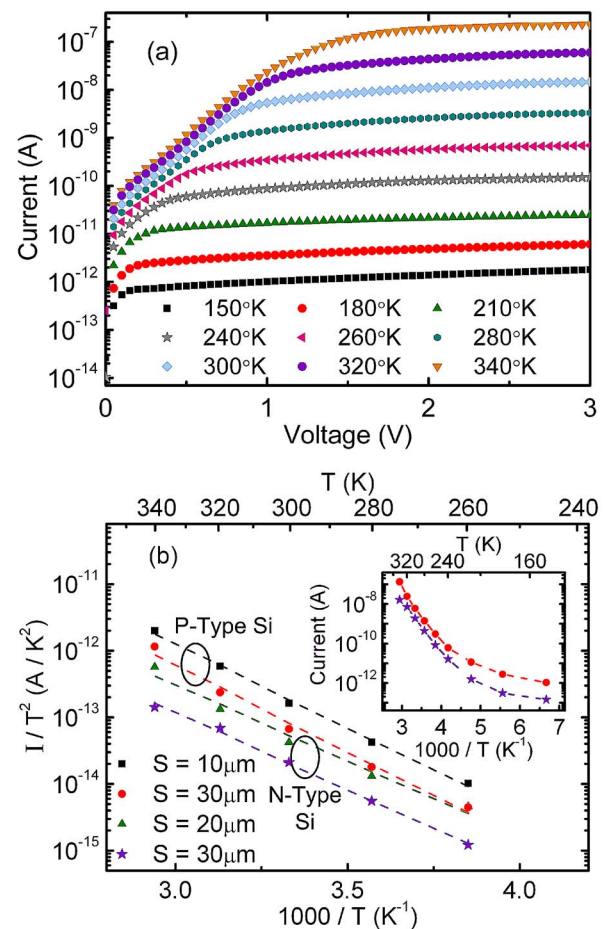


FIG. 3. (Color online) (a) Log current vs applied voltage measured at nine different temperatures between 150 and 340 K for a CNT film-*p*-type Si MSM device with  $W=5\ \mu\text{m}$ ,  $S=10\ \mu\text{m}$ , and  $FL=FW=300\ \mu\text{m}$ . (b) The Richardson plot of  $\log I/T^2$  vs  $1/T$  at  $V=3\ \text{V}$  bias in the temperature range of 260–340 K for four CNT film-Si MSM devices of identical active area ( $FL=FW=300\ \mu\text{m}$ ) and finger width ( $W=5\ \mu\text{m}$ ), but different finger spacing  $S$  and different Si doping types, as labeled in the figure. The dashed lines are linear best fits to the experimental data, from the slope of which Schottky barrier heights of  $\phi_{B_n}=0.45$  and  $0.46\ \text{eV}$  are extracted for  $S=20$  and  $30\ \mu\text{m}$  *n*-type Si devices, and  $\phi_{B_p}=0.50$  and  $0.52\ \text{eV}$  are extracted for  $S=10$  and  $30\ \mu\text{m}$  *p*-type Si devices, respectively. The inset shows log current vs  $1/T$  for the *n*-type and *p*-type Si MSM structures with  $S=30\ \mu\text{m}$  in a wider temperature window (from 150 to 340 K) at  $V=3\ \text{V}$  bias.

the Richardson plots for two *n*-type Si and two *p*-type Si MSM devices with CNT film electrodes in the temperature range of 260–340 K at 3 V voltage bias. From the slopes of Richardson plots for eight *n*-type Si and five *p*-type Si MSM structures, an electron barrier height of  $\phi_{B_n}=0.45 \pm 0.03\ \text{eV}$  and a hole barrier height of  $\phi_{B_p}=0.51 \pm 0.04\ \text{eV}$  were extracted, respectively, showing that thermionic emission dominates the current transport in this temperature range. Furthermore, the type of carriers responsible for conduction in *n*- and *p*-type Si devices were confirmed as electrons and holes, respectively, by measuring the  $I$ - $V$  characteristics of MSM structures with asymmetric electrode areas.<sup>13</sup> Under the assumption that the Fermi level is not pinned, the work function of the CNT film was determined to be  $\phi_M=4.50 \pm 0.03\ \text{eV}$  and  $\phi_M=4.66 \pm 0.04\ \text{eV}$  from the *n*-type and *p*-type Si MSM device measurements, respectively. These values are in good agreement with the previously reported CNT work function values,<sup>14,15</sup> and the value we have extracted from CNT film-GaAs junctions.<sup>10</sup>

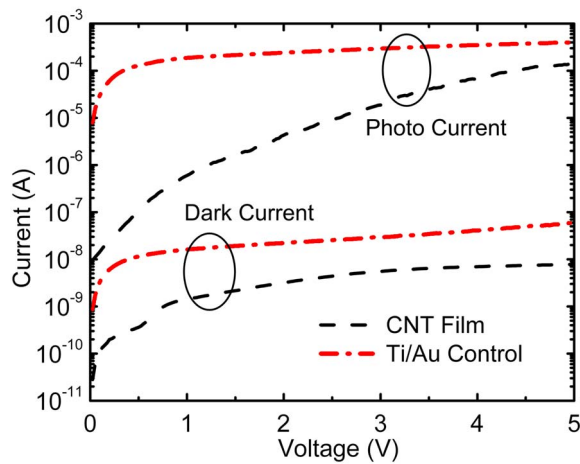


FIG. 4. (Color online) Measured room-temperature dark and photocurrent (log scale) vs applied voltage for MSM devices with CNT film and Ti/Au metal electrodes, as labeled in the figure. For both devices,  $W=5\ \mu\text{m}$ ,  $S=15\ \mu\text{m}$ , and  $FL=FW=300\ \mu\text{m}$  and Si is  $p$ -type.

It is worth noting that the barrier height and work function values reported here include the effect of Schottky barrier lowering since they have been extracted at high bias. Furthermore, the dedoping of the film during the fabrication process<sup>3,4</sup> most likely reduces the extracted work function value. As a result, measurements on isolated  $M$ - $S$  junctions in a controlled environment are necessary for a more accurate determination of the zero-bias barrier heights and the effect of film doping and dedoping on its work function. The inset of Fig. 3(b) shows  $\log I$  versus  $1/T$  for one  $p$ -type Si and one  $n$ -type Si device in the temperature range of 150–340 K. The saturation of the current at temperatures below 240 K suggests that tunneling, which depends weakly on temperature, becomes the dominant current transport mechanism across the CNT film-Si junction at lower temperatures.<sup>16</sup>

For demonstrating the operation of CNT film-Si MSM structures as photodetectors, we also characterized their photoresponse using a standard optical bench equipped with a 633 nm beam scan HeNe laser (6.5 mW power,  $\sim 830\ \mu\text{m}$  spot size) and compared it to the photoresponse of metal control samples. Metal control samples were fabricated following the same process steps used for the CNT film devices, except e-beam evaporated Ti/Au (30/70 nm) metal electrodes were deposited instead of CNT film electrodes. Figure 4 shows the dark and photo  $I$ - $V$  curves for the CNT film and Ti/Au control  $p$ -type Si MSM devices with identical dimensions. Both the dark and photocurrent of the CNT film MSM device is seen to be lower compared to the Ti/Au control. As the Schottky barrier height  $\phi_{B_p}$  between Ti and Si is not smaller than that between the CNT film and Si,<sup>17,18</sup> the lower dark current of the CNT film device is most likely the result of the smaller effective contact area between the mesh of nanotubes making up the porous CNT film and the Si substrate. It is also evident from Fig. 4 that at high voltages, the photocurrent of the CNT film MSM device approaches to that of the Ti/Au control, resulting in a comparable responsivity and a higher photocurrent-to-dark current ratio. Re-

sponsivity and photocurrent-to-dark current ratio normalized to input optical power (NPDR)<sup>19</sup> values extracted for the CNT film-Si MSM device at  $V=5\ \text{V}$  are  $0.133\ \text{A/W}$  and  $1.71 \times 10^4\ \text{mW}^{-1}$ , respectively. The stronger increase in the photocurrent of the CNT film MSM device compared to the Ti/Au control is most likely because of more defects at the CNT film-Si interface, which result in Schottky barrier lowering.<sup>13</sup>

In conclusion, we have characterized the contact between CNT film and silicon by fabricating MSM structures with CNT film electrodes. We have found that at temperatures above  $\sim 240\ \text{K}$ , thermionic emission with  $\phi_{B_n}=0.45\ \text{eV}$  and  $\phi_{B_p}=0.51\ \text{eV}$  is the dominant transport mechanism in CNT film- $n$ -type and  $p$ -type Si junctions, respectively, whereas at lower temperatures tunneling begins to dominate. Furthermore, CNT film MSM devices exhibit a higher photocurrent-to-dark current ratio at high applied voltages relative to metal control devices. Our results provide insight into the fundamental electronic properties of the CNT film-Si junction, which is crucial for any Si-based electronic and optoelectronic devices where the CNT film might be used as a transparent and conductive electrode.

This work was funded in part by the UF Research Opportunity Fund. The authors thank Professor Andrew Rinzler and Zhuangchun Wu for providing the CNT films. They also thank Professor Scott Thompson for the use of his low temperature probe station.

- <sup>1</sup>Z. Wu, Z. Chen, X. Du, J. Logan, J. Sippel, M. Nikolou, K. Kamaras, J. Reynolds, D. Tanner, A. Hebard, and A. Rinzler, *Science* **305**, 1273 (2004).
- <sup>2</sup>G. Grüner, *J. Mater. Chem.* **16**, 2533 (2006).
- <sup>3</sup>A. Behnam, L. Noriega, Y. Choi, Z. Wu, A. G. Rinzler, and A. Ural, *Appl. Phys. Lett.* **89**, 093107 (2006).
- <sup>4</sup>A. Behnam, Y. Choi, L. Noriega, Z. Wu, I. Kravchenko, A. G. Rinzler, and A. Ural, *J. Vac. Sci. Technol. B* **25**, 348 (2007).
- <sup>5</sup>S. Lu and B. Panchapakesan, *Appl. Phys. Lett.* **88**, 253107 (2006).
- <sup>6</sup>K. Lee, Z. Wu, Z. Chen, F. Ren, S. J. Pearton, and A. G. Rinzler, *Nano Lett.* **4**, 911 (2004).
- <sup>7</sup>M. C. Aguirre, S. Auvray, S. Pigeon, R. Izquierdo, R. Desjardins, and R. Martel, *Appl. Phys. Lett.* **88**, 183194 (2006).
- <sup>8</sup>A. D. Pasquier, H. E. Unalan, A. Kanwal, S. Miller, and M. Chhowalla, *Appl. Phys. Lett.* **87**, 203511 (2005).
- <sup>9</sup>M. W. Rowell, M. A. Topinka, M. D. McGehee, H. J. Prall, G. Dennler, N. S. Sariciftci, L. Hu, and G. Grüner, *Appl. Phys. Lett.* **88**, 233506 (2006).
- <sup>10</sup>A. Behnam, J. L. Johnson, Y. Choi, L. Noriega, M. G. Ertoşun, Z. Wu, A. G. Rinzler, P. Kapur, K. C. Saraswat, and A. Ural, *J. Appl. Phys.* **103**, 114315 (2008).
- <sup>11</sup>S. M. Sze, D. J. Coleman, and A. Loya, *Solid-State Electron.* **14**, 1209 (1971).
- <sup>12</sup>B. Majkusiak, *IEEE Trans. Electron Devices* **45**, 1903 (1998).
- <sup>13</sup>J. Burm and L. F. Eastman, *IEEE Photonics Technol. Lett.* **8**, 113 (1996).
- <sup>14</sup>V. Barone, J. E. Peralta, J. Uddin, and E. S. Gustavo, *J. Chem. Phys.* **124**, 024709 (2006).
- <sup>15</sup>B. Shan and K. Cho, *Phys. Rev. Lett.* **94**, 236602 (2005).
- <sup>16</sup>E. J. Miller, E. T. Yu, P. Waltereit, and J. S. Speck, *Appl. Phys. Lett.* **84**, 535 (2004).
- <sup>17</sup>M. O. Aboelfotoh, *J. Appl. Phys.* **64**, 4046 (1988).
- <sup>18</sup>We have extracted slightly higher  $\phi_{B_p}$  values for the control samples compared to those for the CNT film samples.
- <sup>19</sup>C. O. Chui, A. K. Okyay, and K. C. Saraswat, *IEEE Photonics Technol. Lett.* **15**, 1585 (2003).